COVER SHEET

Y. Chen, X. Miao, "Thermal and chemical stability of fluorohydroxyapatite ceramics with different fluorine contents", *Biomaterials,* 26[11] (2005), pp. 1205-1210.

Thermal and chemical stability of fluoro-hydroxyapatite ceramics with different fluorine contents

Yanming Chen, Xigeng Miao*

School of Materials Engineering, Nanyang Technological University, Nanyang Avenue, 639798, Singapore

Abstract

Hydroxyapatite (HA) plays an important role in orthopedics and dentistry due to its excellent bioactivity. However, the thermal decomposition and the poor corrosion resistance in an acid environment have restricted the applications of hydroxyapatite. In this study several fluorine-substituted hydroxyapatite (FHA) ceramics with the general chemical formula of $Ca_{10}(PO_4)_6(OH)_{2-2x}F_{2x}$, where x = 0.0, 0.2, 0.4, 0.6, 0.8, 1.0, were prepared. Thermogravimetric analysis in the temperature range from 25°C to 1400°C showed that the FHA ceramics with x > 0.4 had remarkably improved thermal stability as compared to pure HA. X-ray diffraction of the FHA ceramics sintered at 1300°C for 1 hour further confirmed the thermal stability. Dilatometer analysis showed that the fluorine addition substantially increased the onset sintering temperature of the FHA ceramics. Density measurements showed that the fluorine addition into the HA matrices slightly retarded the densification of the FHA ceramics. Corrosion testing on the polished surfaces of the FHA ceramics using a 2.5 wt% citric acid solution indicated that the FHA ceramics with $x \geq 0.4$ had substantially improved corrosion resistance.

Keywords: Hydroxyapatite; Fluoroapatite; Stability

* Corresponding author.
E-mail address: asxgmiao@ntu.edu.sg (X. Miao); fax: (65) 6790 9081

1. Introduction

Synthetic hydroxyapatite (HA; $Ca_{10}(PO_4)_6(OH)_2$) has been extensively investigated as a bone substitute material due to its similar chemical composition to that of bone, its direct bone bonding ability, and its commercial availability. However, synthetic hydroxyapatite presents poor thermal stability indicated by the decomposition into other phases such as tricalcium phosphate (TCP; $Ca_3(PO_4)_2$) at sintering temperatures higher than 1200°C. This phase impurity often results in undesirable fast dissolution rate in *vivo*. The lack of commercially efficient techniques in processing pure hydroxyapatite ceramics to full densification without decomposition has somewhat restricted the wider applications of hydroxyapatite ceramics. Moreover, even pure hydroxyapatite ceramics such as those prepared by hot pressing show too high a dissolution rate in biological environments. This high dissolution rate presents a long-term performance problem of HA coatings on ceramic or metallic implants used for cases such as dental roots and fastening nails for fracture bones. On the other hand, fluoroapatite as an apatite exhibits high thermal stability and can retain its phase purity

up to a temperature of 1400^{o}C [1]. Since the fluorine content in pure fluoroapatite (3.77 wt %) is much higher than that in human bone (<1.00 wt %), the toxicity of fluoroapatite after implantation needs to be considered. It was reported by Lugscheider et al. [2] that no cytotoxic influence on cells in culture could be detected. Extremely low dissolution rate of fluoroapatite in biological environments was also reported [3]. Nevertheless, fluoroapatite alone may not be a good biomaterial because it is too stable (or too bioinert) and thus lacks good biological properties [4, 5]. For practical applications, the mechanical properties, bioactivity, biostability, and biodegradability should be tailed for particular situations. In fact, bioactive/biodegradable and functionally graded composites have been reported to achieve comprehensive properties [6].

Recently, partially fluorine-substituted hydroxyapatite (FHA; $Ca_{10}(PO_4)_6(OH)_{2-2x}F_{2x}$, $0<x<1$) has attracted much attention due to the extensive findings of partially fluoridated hydroxyapatite in bone and teeth and due to the favorable effect of fluoride on bone growth [7]. Many methods have been developed, namely, solid state reaction, wet precipitation, and sol-gel processing for the preparation of FHA powders and ceramics [8-10]. Various preparation parameters have also been investigated for the wet precipitation and the sol-gel processing methods [8-12]. However, most studies so far have focused on the preparation of FHA powders. The effects of different fluorine contents on the thermal property and the corrosion resistance of FHA ceramics have seldom been studied systematically. Therefore, in the present study, nanosized FHA powders with different fluorine contents were prepared by a wet precipitation method. The powders were then calcined, pressed and sintered at 1300^{o}C in air. Subsequently, the effects of fluorine contents on the thermal stability (resistance to decomposition) and the chemical stability (corrosion resistance) of FHA ceramics were investigated.

2. Experimental procedure

2.1 Sample preparation

Calcium nitrate 4-hydrate ($Ca(NO_3)_2{\cdot}4H_2O$, AnalarR grade, BDH Limited Company, Inc.), diammonia hydrogen phosphate ($(NH_4)_2HPO_4$, Merck KgaA Company, Inc.) and ammonia fluoride (NH_4F, Fluka Chemie Company, Inc.) were used as the starting chemicals. The sample preparation was performed in a fume cupboard installed in an air-conditioned laboratory, with the room temperature set at 25 ^{o}C. For the preparation of pure HA, fluorine-substituted HA (FHA), and pure FA powders, 0.5 M calcium nitrate 4-hydrate was first dissolved in distilled water followed by adding diammonia hydrogen phosphate aqueous solution dropwise to achieve the Ca/P ratio of 1.67. Then ammonia fluoride solution was added into the constantly stirred Ca and P containing solution. Different amounts of ammonia fluoride solution were added individually to control the value x in the general formula of $Ca_{10}(PO_4)_6(OH)_{2-2x}F_{2x}$. When the x was 0, 0.2, 0.4, 0.6, 0.8, and 1.0, respectively, the subsequently obtained powders and ceramics were named HA, HA02F, HA04F, HA06F, HA08F, and FA, respectively. To obtain the precipitates, an ammonia solution was dropped into the mixed solution to obtain pH 10-11, followed by constant stirring for 2 hours. The suspension with the precipitates was then kept still for 24 hours before the supernatant solution was discarded and the precipitates were washed several times with distilled water to remove the residual ions. The washed precipitates were dried in air and crushed by ball milling with ethanol for 1 hour, followed by drying again in oven. The pieces of dried powder cakes were then ground into fine

powders using a vibrating dry mill. The formed powders were then calcined at 700^{o}C for half an hour in a furnace, followed by dry milling and pressing at 200MPa in a steel die. One batch of the pressed pellets was sintered in air at 1300^{o}C for 1 hour with a heating rate of 5^{o}C/min and a cooling rate of 10^{o}C/min.

2.2 Sample characterization

The FHA powders and the sintered FHA ceramics were characterized using x-ray diffraction (XRD, Lab XRD-6000 Shimadzu). XRD data of the FHA powders and the sintered FHA bodies were collected from 20^{o} to 60^{o} (two theta angle) using the monochromatic CuKα radiation at the step of 0.02^{o} with a counting time of 1 second per step. A batch of the uncalcined FHA powders was heated in a thermogravimetric analyzer (TGA, Rheometric Scientific) in the temperature range from 25^{o}C to 1400^{o}C. A batch of the pressed pellets was heated to 1450^{o}C at a heating rate of 5^{o}C/min in a horizontal dilatometer (Unitherm Model 1161 High-Temperature Dilatometer System) to obtain the sintering shrinkage data. The FHA ceramics sintered at 1300^{o}C for 1 hour were polished and immersed in a 2.5wt% citric acid solution for 10 minutes, followed by examination under a scanning electron microscope (SEM; JOEL, JSM-5410 LV) to compare the surface morphologies before and after chemical corrosion. The bulk densities of the FHA ceramics sintered at 1300 ^{o}C for 1 hour were calculated using the formula of density = weight / volume, where the volume of a sample was measured by a micrometer and also a densometer based on the Archimedes principle.

3. Results and discussion

The as-prepared and uncalcined HA, FHA, and FA powders were all elongated in particle shape with about 80nm in length and 20nm in width. The as-prepared and uncalcined powders also showed poor crystallinity due to the broad XRD peaks observed. However, calcination was used in this study to increase the crystallinity and remove the absorbed water on the as-prepared powders without significantly increasing the particle sizes. Fig. 1 shows the XRD patterns of the as-prepared HA, FHA, and FA powders subjected to calcination at 700^{o}C. Some sets of peaks (reflections) gradually shifted to the right hand side with the increase of the fluorine content. For example, the (3 0 0) reflections of the HA, HA02F, HA04F, HA06F, HA08F, and FA powders occurred gradually at higher two theta angle with the fluorine content, namely, at 32.84^{o}, 32.98^{o}, 33.06^{o}, 33.08^{o}, 33.10^{o}, and 33.14^{o}, respectively. The slight shift of the characteristic (300) peaks to the right side of the two-theta axis was related to the decrease of the a-axis length of the hexagonal HA crystal lattice. This observation was in agreement with the fact that fluorine addition tends to decrease the lattice parameter a, but not obviously affect the lattice parameter c. From Fig. 1, one can see that the shape of the peaks of the fluoride-substituted HA was sharper than that of pure HA. Thus, it can be seen that the incorporation of fluorine into the HA matrix did increase the crystallinity of the host crystals. The increased crystallinity corresponded to the increased thermal and chemical stability of the FHA ceramics, as will be discussed later.

Thermogravimetric analysis data of the as-prepared and uncalcined FHA powders (loosely packed in an alumina crucible) in the temperature range from 25^{o}C to 1400^{o}C were used to determine the onset temperatures of the loss of OH^{-} groups and the decomposition of the HA, FHA, and FA powders. Fig. 2 shows different degrees of weight loss of the samples with respect to different

fluorine contents. It can be seen that pure HA sample had three stages of weight loss; the first stage from 25°C to 200°C was due to the evaporation of absorbed water in the fine powder, the second stage from 800°C to 850°C was due to the release of OH^- groups from the HA crystals, and the third stage above 1000°C was related to the further decomposition of HA and hence the large loss of the OH^- groups. This observation of weight loss during the heating process was in agreement with the decomposition sequence described by E. Adolfsson et al. [10], who reported that the decomposition reactions of HA could be divided into two steps, according to the formulae below:

$$Ca_{10}(PO_4)_6(OH)_2 \rightarrow Ca_{10}(PO_4)_6(OH)_{2-2x}O_x + xH_2O \quad \text{(at about 800 °C)} \quad (1)$$

$$Ca_{10}(PO_4)_6(OH)_{2-2x}O_x \rightarrow 3Ca_3(PO_4)_2 + CaO + (1-x)H_2O \quad \text{(at about 1220 °C)} \quad (2)$$

However, only the first stage and the second stage could be observed in the HA02F sample. Moreover, for all the FHA samples with fluorine contents higher than that in the HA02F sample, only the first stage could be detected. These observations suggested that when the fluorine content in the HA matrix was high enough, the thermal stability of the HA matrix would be greatly increased or the decomposition of the HA matrix would be effectively retarded. While the increase of thermal stability with fluorine content was well demonstrated, the weight loss at the first stage varied from one powder sample to another, as was shown by the large weight loss of the HA02F powder. This discrepancy could be explained by the humidity of the air and the storage of the different powder samples, which incidentally resulted in the large amount of water absorbed on the HA02F powder.

The sintering shrinkage (i.e., the relative shrinkage) and the sintering shrinkage rate data were acquired by sintering the pressed HA and FA pellets in the dilatometer from 25°C to 1450°C, as shown in Fig. 3. From the sintering shrinkage rate data, one can see that the onset sintering temperature of HA was around 1000°C. Within the temperature range from 1000°C to 1100°C, the sintering shrinkage rate or the densification rate increased rapidly. At 1100°C a maximum densification rate was reached. In the temperature range from 1100°C to 1450°C, the densification rate was gradually slowed down to zero. On the other hand, for the pressed FA sample, the onset sintering temperature was about 1150°C. Within the temperature range from 1150°C to 1250°C, the densification rate increased sharply. At 1250°C the highest densification rate was obtained, and the sintering process was completed near 1450°C. Thus, the onset sintering temperature of 1000°C and the highest densification rate temperature of 1100°C of HA pellet were significantly lower than those of FA pellet. This observation could be ascribed to the low atomic or ionic diffusion rate in FA pellet, caused by the strong inter-atomic bonding between the fluorine ions and the other ions in the HA matrix. The low tendency of decomposition and the high densification temperature of FA, as shown in Fig. 2 and Fig. 3 respectively, suggested the high thermal stability of FA and FHA ceramics, as compared to pure HA ceramics. The thermal stability of FA and FHA ceramics could be related to their increased crystallinity and the strong ionic bonding in the crystal structures.

The XRD patterns of the HA, FHA, and FA ceramics sintered at 1300°C in air are shown in Fig. 4. It can be seen that severe decomposition of HA to β-TCP occurred in the pure HA sample as a result of the sintering process. Since β-TCP phase is a low temperature TCP phase, the β-TCP phase detected must be derived from the high temperature α-TCP phase through the α-TCP to β-TCP phase transformation. Although the degree of decomposition was much reduced in the HA02F and HA04F samples, the amount of β-TCP phase formed was still substantial. However, in the HA06F

sample and in the FHA samples having fluorine contents higher than that in HA06F, the decomposition was dramatically suppressed. This observation again agreed with the previous result that above a certain fluorine content, the FHA ceramics exhibited high thermal stability. In this study, the HA matrices in the FHA ceramics were regarded as relatively stable when the x in the general FHA formula was greater than 0.6.

While the bulk densities of the FHA ceramics were easily determined, the determination of the relative densities of the FHA ceramics was not a simple task. The FHA ceramics were not phase pure and thus the contents of the FHA apatite phase and the β-TCP phase should be determined. This phase content determination was additionally conducted using an external standard method, in which the XRD reflection intensity ratios were correlated with the preset contents of the powder mixtures of the FHA apatite phase and the β-TCP phase. On the other hand, accurate measurements of the theoretical densities of the FHA apatite phase and the β-TCP phase were not done through the crystal lattice analysis due to the large amounts of calculations required. Since the published theoretical densities of pure HA and pure FA ceramics are very similar, 3.16g/cm^3 and 3.10-3.20 g/cm^3, respectively, the theoretical densities of the FHA ceramics were simply taken as 3.13g/cm^3. Similarly, the reported theoretical density of 3.00 g/cm^3 of the β-TCP phase was taken in this study, regardless of the fluorine content in the β-TCP phase.

Given the phase ratios and the theoretical densities of the two phases, the theoretical densities of the FHA ceramics were calculated based on the rule of mixture. It was finally found that the relative densities gradually and almost linearly decreased from 96% for pure HA ceramics to 93 % for pure FA ceramics. These levels of relative densities were regarded as high due to the short sintering time of 1 hour used at 1300 ^{o}C. Cautiously speaking, it seemed that the fluorine addition slightly retarded the densification process and decreased the relative densities of the FHA ceramics, which fortunately agreed with the sintering shrinkage data from the dilatometer (Fig. 3). The residual porosities due to the remaining micropores of the HA, FHA, and FA ceramics were confirmed by SEM observations of polished surfaces. The micropores due to the incomplete sintering were different from those surface defects as a result of chemical attack occurring during the chemical stability test.

A batch of HA, FHA, and FA ceramics was polished and the polished surfaces were immersed in a 2.5 wt% citric acid solution for 10 minutes before the surfaces were rinsed, dried, and examined under SEM. The surface morphologies after the chemical attack are shown in Fig. 5. For the samples with fluorine contents corresponding to $x \leq 0.4$, the surfaces were severely damaged; zones of grains and phases were dissolved. Meanwhile, for the samples with fluorine contents corresponding to $x > 0.4$, the surfaces appeared to be much smoother; only the grain boundaries were slightly etched. These observations indicated that when the fluorine content in the FHA ceramics reached a certain high level (i.e., when $x = 0.6$), the corrosion resistance of the ceramics was greatly improved.

It should be noted that the pores or the defects on the chemically attacked surfaces were due to three factors: one was the remaining micropores due to the incomplete densification; one was the remaining β-TCP phase as the decomposition product, which was dissolved much faster than the pure HA phase; the other was the intrinsic chemical stability of the FHA ceramics and especially the

FA ceramics. Different degrees of chemical attack certainly occurred on the polished surfaces as the sintered FA ceramic was found to be more porous than the sintered HA ceramic sample. From Fig. 4 and judging from the XRD peak ratios, one can see that the β-TCP phase increased in amount from FA to HA samples. This trend agreed with the increased amounts of surface defects on the surfaces from FA to HA samples, as shown in Fig. 5. Thus, the β-TCP phase could be the dominant factor causing the surface damage. Nevertheless, the formation of β-TCP was directly related to the content of added fluorine. The final issue was the intrinsic higher chemical stability of the FHA and the FA samples than the pure HA samples, as was proved by our previous corrosion tests with the HA, FAH, and FA ceramics sintered at 1200 ^{o}C, at which no β-TCP was formed.

It was found in this study that there existed a certain fluorine content above which the FHA ceramics showed substantially improved thermal and chemical stability. This phenomenon could be explained by considering the crystal structure of HA. As shown in Fig. 6, the hydrogen (H^{+}) ions (the smallest spheres in the figure) of HA were arranged in the atomic interstices neighboring to the oxygen ions (O^{2-}), forming OH^{-} groups and were oriented randomly, which conferred a certain degree of disorder to the crystal structure of HA. Once the OH^{-} groups were partially substituted by the F^{-} ions, the existing hydrogen ions of the OH^{-} groups were bound to the nearby F^{-} ions because of the higher affinity of the F^{-} ions in respect to the oxygen ions, producing a quite well-ordered apatite structure, which caused the increase of the thermal and chemical stability of the HA matrix. Therefore, when a certain amount of F^{-} ions substituted the OH^{-} groups in the HA matrix, a certain level of chemical and thermal stability of the FHA ceramics was achieved. Theoretically, the F^{-} ion concentration of 50% in the FHA should be enough to remove the disorder of the crystal structure of HA and hence stabilize the structure due to the alternating arrangement of the F^{-} ions between each pair of OH^{-} groups. However, by considering the random substitution of OH^{-} ions with F^{-} ions in the OH^{-} positions, the F^{-} ion concentration required to stabilize the structure was necessarily higher than 50%. In this study, the F^{-} ion concentration was observed to be about 60%.

5. Conclusion

Nanosized FHA powders with different fluorine contents were prepared by a wet precipitation method. XRD data of the FHA ceramics sintered at 1300^{o}C and TGA data of the FHA powders in the temperature range from 25^{o}C to 1300^{o}C, revealed that when the fluorine content was higher than the composition of x = 0.6 in the $Ca_{10}(PO_4)_6(OH)_{2-2x}F_{2x}$ formula, the thermal stability of the HA matrix was substantially increased and the decomposition of the HA matrix was effectively restrained. On the other hand, sintering shrinkage data from the dilatometer showed that when a certain amount of fluorine was introduced into the HA matrix, the onset sintering temperature was substantially increased. In addition, the measured densities of the FHA ceramics showed that the fluorine addition had slightly negative effect on the densification process of the FHA ceramics. Finally, corrosion testing with the citric acid solution showed a similar tendency of chemical stability; the FHA ceramics with fluorine contents corresponding to $x \geq 0.6$ had greatly improved corrosion resistance.

Acknowledgment

The authors would like to thank the Nanyang Technological University for the provision of the financial support (AcRF RG26/01).

References

1. Wei M, Evans JH. Synthesis and characterization of hydroxyapatite and fluorapatite. Key Engineering Materials 2002; 218-220: 35-38.
2. Lugscheider E, Knepper M, Heimberg B, Dekker A, Kirkpatrick CJ. Cytotoxicity investigations of plasma sprayed calcium phosphate coatings. J. Mater. Sci.: Mater. Med. 1994; 5: 371-375.
3. Adolfsson E, Nygren M, Hermansson L. Decomposition mechanisms in aluminum oxide-apatite systems. J. Am. Ceram. Soc. 1999; 82: 2909-2912.
4. Downes S, Clifford CJ, Scotchford C, Klein CPAT. Comparison of the release of growth hormone from hydroxyapatite, heat-treated hydroxyapatite, and fluoroapatite coatings on titanium. J. Biomed. Mater. Res. 1995; 29: 1053-1060.
5. Dhert WJA, Klein CPAT, Wolke JGC, van der Velde EA, de Groot K, Rozing P M. Mechanical investigation of fluorapatite, magnesiumwhitlockite, and hydroxylapatite plama-sprayed coatings in goats. J. Biomed. Mater. Res. 1991; 25: 1183-1200.
6. Wong LH, Tio B, Miao X. Functionally graded tricalcium phosphate/fluoroapatite composites. Materials Science and Engineering C 2002; 20:111-115.
7. Wei M, Vellinga D, Leavesley D, Evans J, Upton Z. Cell attachment and proliferation on hydroxyapatite and ion substituted hydroxyapatites. Key Engineering Materials 2003; 240-242:671-674.
8. Jha LJ, Best SM, Knowles JC, Rehman I, Santo JD, Bonfield W. Preparation and characterization of fluoride-substituted apatites. J. Mater. Sci.: Mater. Med. 1997; 8: 185-191.
9. Rodriguez-Lorenzo LM, Hart JN, Gross KA. Influence of fluorine in the synthesis of apatites. Synthesis of solid solutions of hydroxy-fuorapatite. Biomaterials 2003; 24: 3777-3785.
10. Okazaki M, Tohda H, Yanagisawa T, Taira M, Takahashi J. Differences in solubility of two types of heterogeneous fluoridated hydroxyapatite. Biomaterials 1998; 19: 611-616.
11. Okazaki M, Miake Y, Tohda H, Yanagisawa T, Takahashi J. Fluoridated apatite synthesized using a multi-step fluoride supply system. Biomaterials 1999; 20: 1303-1307.
12. Okazaki M, Miake Y, Tohda H, Yanagisawa T, Matsumoto T, Takahashi J. Functionally graded fluoridated apatites. Biomaterials 1999; 20: 1421-1426.

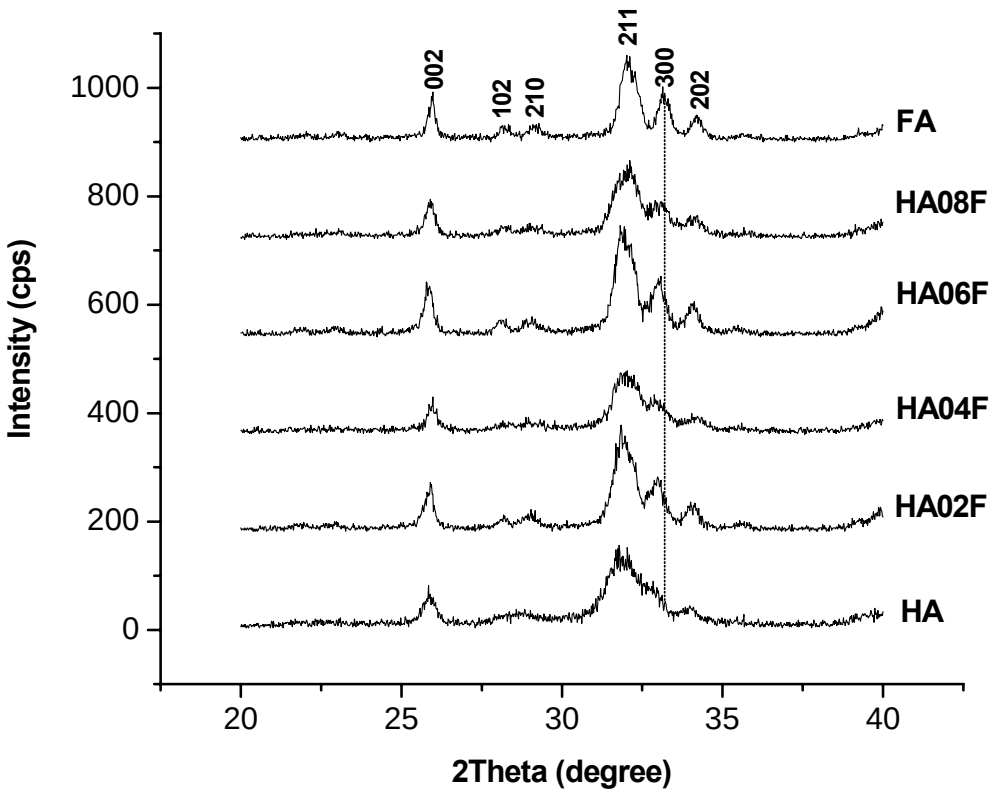

Fig. 1. XRD patterns of HA, FHA and FA powders after calcination at 700^{o}C.

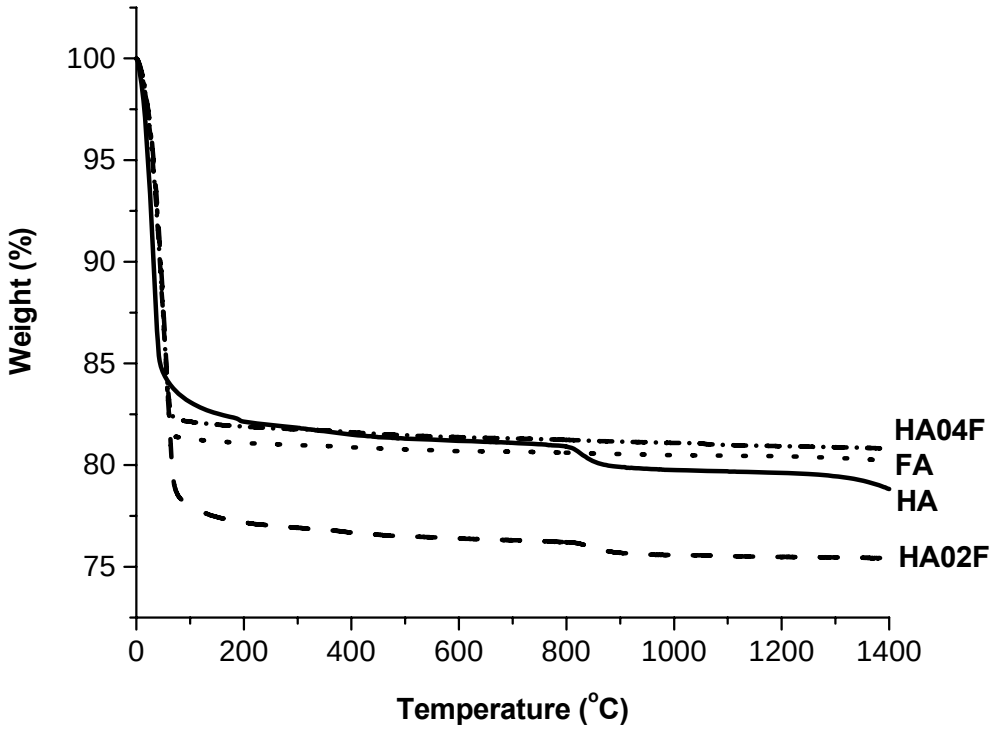

Fig. 2. TGA data of HA, FHA and FA powders heated to 1400°C in dry air.

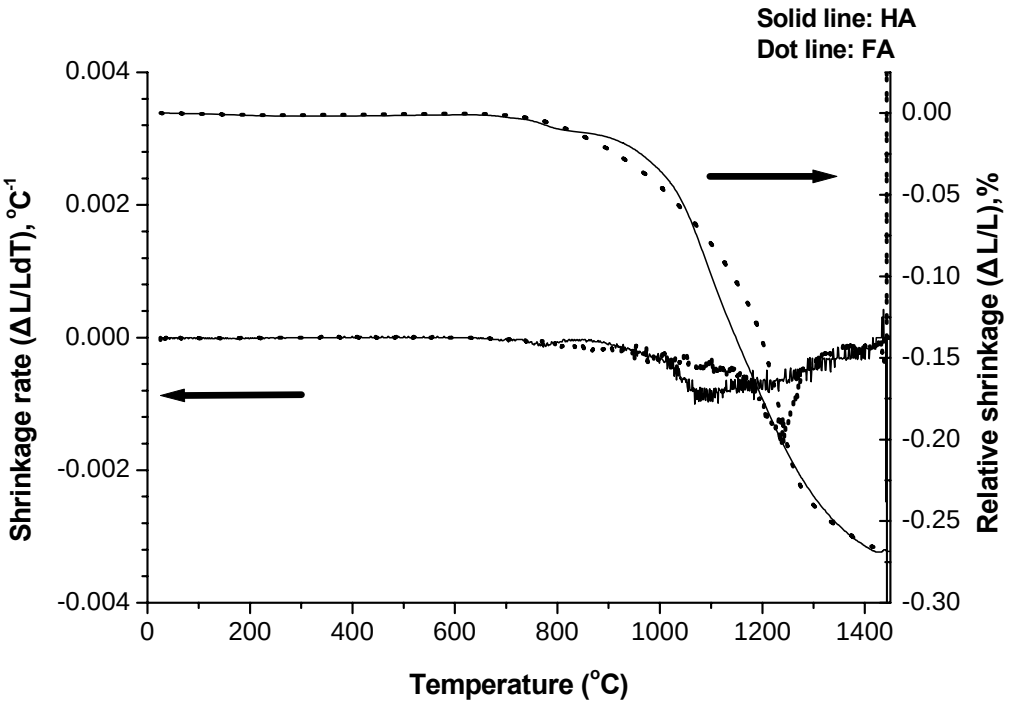

Fig. 3. Shrinkage and shrinkage rate data of HA and FA sintered up to 1450°C.

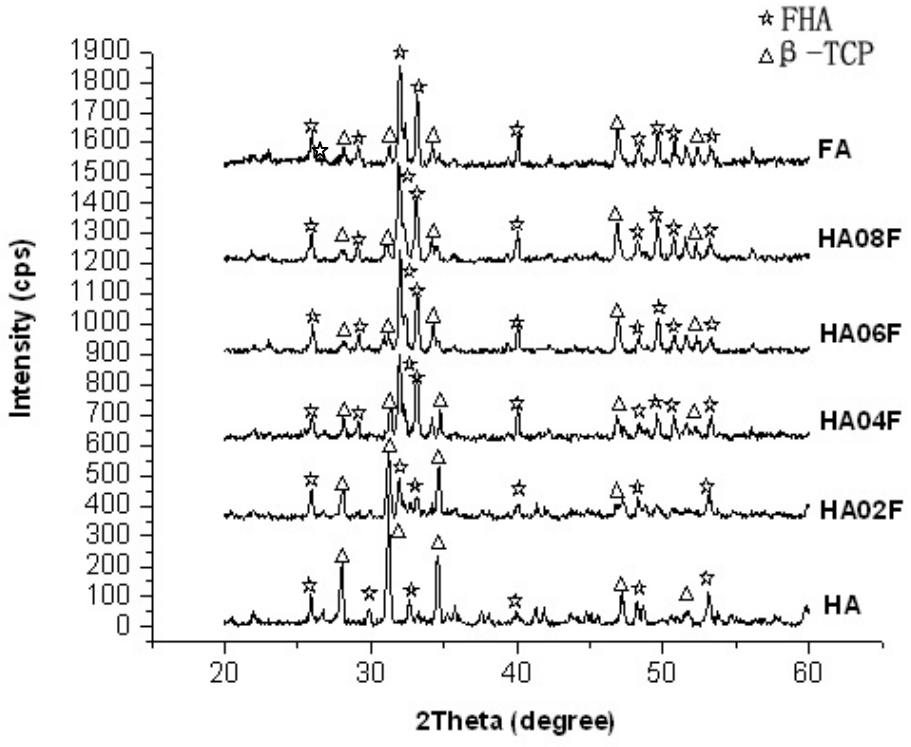

Fig. 4. XRD patterns of HA, FHA, and FA ceramics sintered at 1300^{o}C in air.

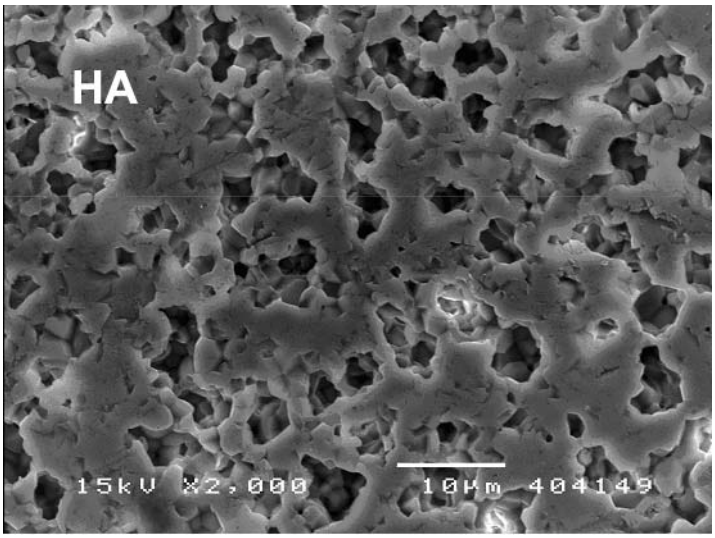
HA
15kV X2,000
10µm 404149

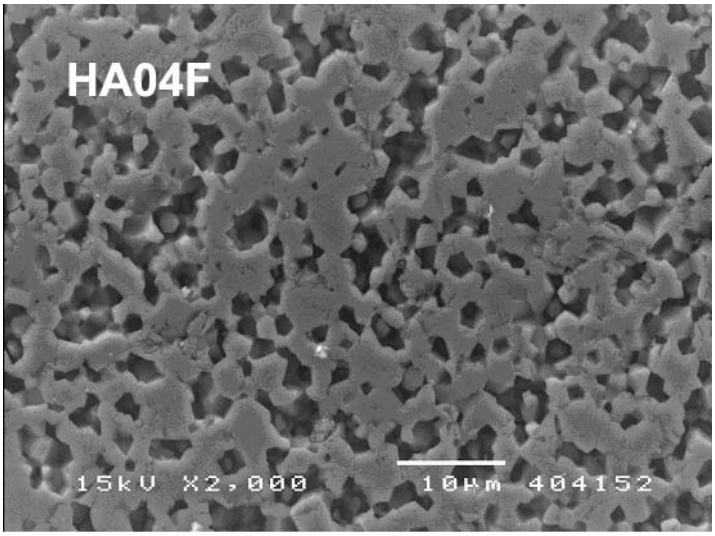
HA04F
15kV X2,000
10µm 404152

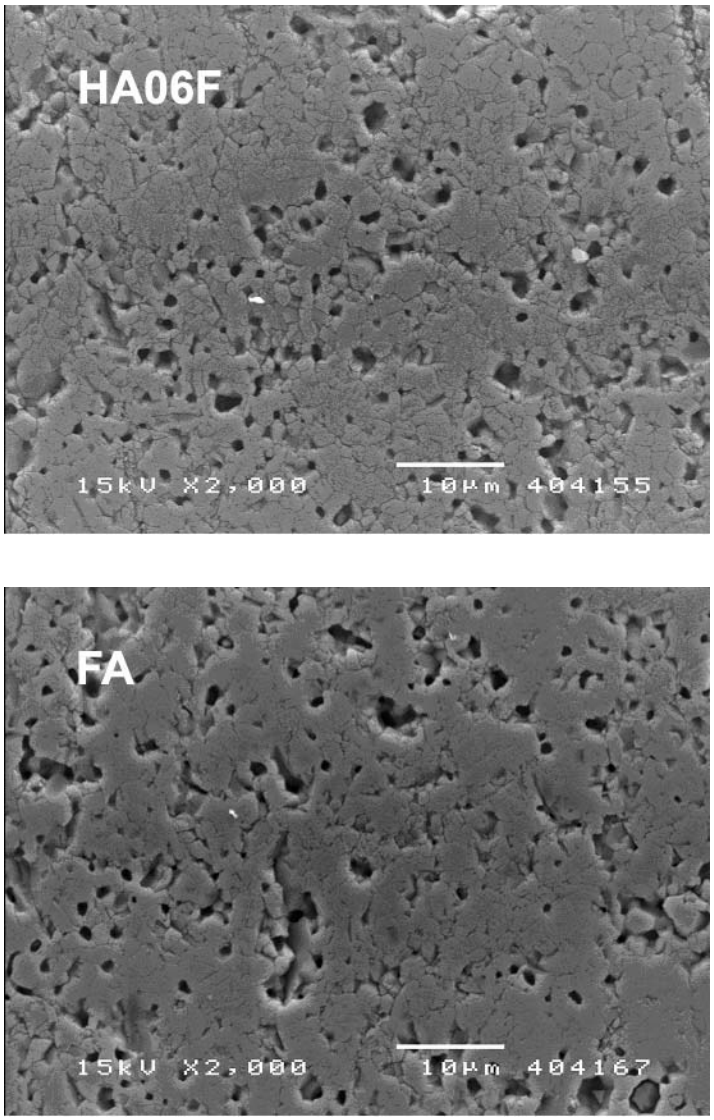

Fig. 5. Surface morphologies of HA, HA04F, HA06F, and FA ceramics sintered at 1300 ^{o}C for 1 hour, followed by polishing and immersion in a 2.5 wt% citric acid solution for 10 minutes.

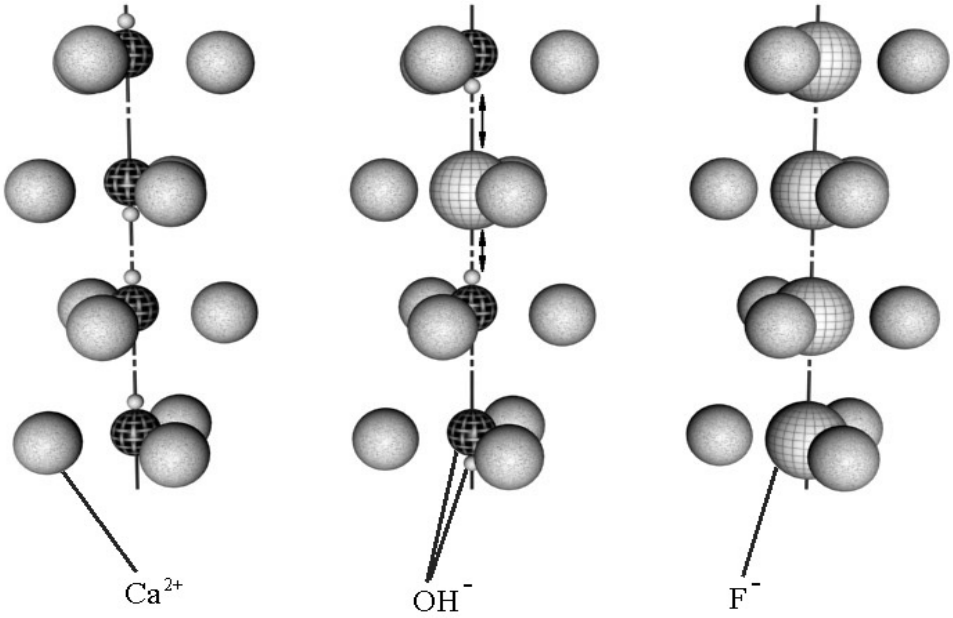

Fig. 6. Arrangement of OH^- groups and F^- ions in HA, FHA, and FA crystal structures.